WCTE 2018
2018 World Conference on Timber Engineering
August 20 - 23, 2018 | Seoul, Republic of Korea

A NOVEL LVL-BASED INTERNAL REINFORCEMENT FOR HOLES IN GLULAM BEAMS

Cristobal Tapia Camú[1], **Simon Aicher**[2]

ABSTRACT: A newly developed reinforcement system for glulam, actually representing a new generic wood compund, is presented. The composite consists on a hybrid cross-section, composed of intercalated layers of GLT and LVL, glued together along the width-direction of the beam. The specific build-up improves in first instance the mechanical properties of the glulam in the direction perpendicular to the grain significantly. Hence, the composite is especially well suited for the reinforcement of arrays of large holes in wide cross-sections. Secondly, the layers were tailored in such a manner, that the bending load capacity equalls that of the gross-cross-section. A parametric study was performed by means of the finite element method, to study the redistribution of stresses perpendicular to the main axis of the beam in the region of stress concentrations at one of the hole corners. Specifically, the load sharing of the vertical tensile force $F_{t,90}$ described in the German National Annex to EC5 was analyzed, and an analytical relationship depending on the thickness, elastic modulus and moment-to-shear-force ratio was developed.

KEYWORDS: holes, LVL, GLT, reinforcements, hybrid build-up, parametric study

1 INTRODUCTION

The drilling of holes in beams made of glued laminated timber (GLT) represents a frequent necessity in timber structures, as they are required for the passing-through of plumbing, electrical and other service-relevant infrastructure systems. These apertures represent size-dependant significant weak sections in the beam. The holes can lead to significant reductions of the cross-section, e.g. up to 40%, and, most importantly, lead to stress concentrations at the hole corners, resulting in a noticeable decrease of the maximum load capacities. The failure mechanism of unreinforced and reinforced holes is well known and is manifested by the propagation of cracks in the direction of the grain and beam-length axis, starting from two zones with high tensile stresses perpendicular to the grain, which are located at diagonally opposite corner areas of the hole.

Typically, two possible types of reinforcements are considered to prevent an early propagation of cracks at the high-stressed corners: internal screw-type reinforcements and external wood panels, both of which can be designed according to the German National Annex to EC5 [1]. The two reinforcement alternatives show different advantages and drawbacks when it comes to their mechanical behavior, ease of application and aesthetics, which play an important role in deciding in favor of one or the other. Regarding the mechanical aspects, externally applied plates outperform in general the screw-type reinforcements, since they are not only able to redirect the stresses perpendicular to the grain, but are also capable to transfer the shear stresses present in the crack-endangered region [2]. Although new investigations show that inclined arrangements of screw-type reinforcements can help in the transmission of shear stresses too [3, 4], their application, as well as for non-inclined reinforcements, is in practice limited to small-to-medium sized beams. Nevertheless, external reinforcements also reveal a mechanical disadvantage, which becomes evident when cross-sections of large thicknesses need to be reinforced. In such a scenario, the panels, fixed on the wide sides of the beam, have little to no influence on the stresses near the mid-width zone, which reduces their effectiveness considerably. Even an increase of the plate's thickness makes no big difference regarding this issue [2].

To overcome this problem, and based on the necessities of a specific building project [5], a novel kind of reinforcement for holes in glulam beams was developed. The approach consists in the application of one or several internal, vertically placed LVL layers between adjacent layers of GLT, creating a special composite element. This hybrid configuration enables the reduction of the peak stresses at the crack-prone corners more effectively, as compared to simple external plates, and has proven to be especially well suited for configurations with multiple large holes placed close to each other [6].

2 TENSILE FORCE PERPENDICULAR TO THE GRAIN $F_{t,90}$

The present design of holes and hole reinforcements according to DIN EN 1995-1-1/NA [1] is based on a fictive resultant tensile force, $F_{t,90}$, representing the integral of

[1] Cristóbal Tapia, MPA, University of Stuttgart, Germany, cristobal.tapia-camu@mpa.uni-stuttgart.de
[2] Simon Aicher, MPA, University of Stuttgart, Germany, simon.aicher@mpa.uni-stuttgart.de

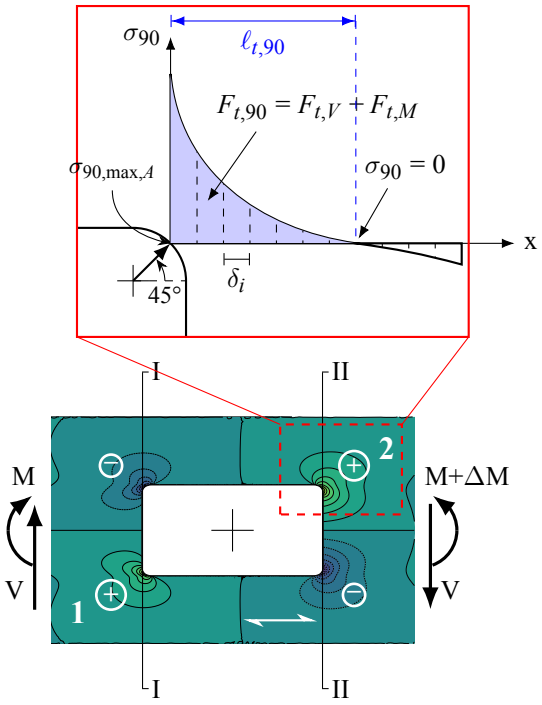

Figure 1: *Definition of the vertical tensile force $F_{t,90}$ shown for the case of a rectangular hole. Regions 1 and 2 are subjected to tensile stresses perpendicular to the grain in the vicinity of the corners of the hole. The colored field depicts the stress-stresses perpendicular to the grain σ_{90}.*

the stresses perpendicular to the grain in the hole periphery in the crack relevant sections (see Figure 1). This force is composed of two additive parts: one, $F_{t,V}$, accounting for the shear force, which cannot be transferred in the hole area, and a second part, $F_{t,M}$, related to the bending moment present in the cross-section:

$$F_{t,90} = F_{t,V} + F_{t,M}. \tag{1}$$

The exact form taken by each of the two terms is, for this paper, not relevant—although discussion about this topic can be found in Refs. [2, 7, 8]. The vertical force acc. to Eq. (1) is used for the design of unreinforced and reinforced holes. In the first case, the force is compared against a fictive resulting resistance force, based on the size-dependent tensile strength of the glulam perpendicular to the grain. In the second case, the force is the basis of the design of reinforcement elements (screws, rods, plates). Since the analyzed reinforcement system is used in combination with holes in GLT beams, the tensile force $F_{t,90}$ becomes a relevant parameter, and is used throughout this paper for the different analysis. For this purpose, finite element results are used to numerically compute the tensile force, following the method depicted graphically in Figure 1 (the exact procedure is explained in Section 4).

3 REINFORCEMENT DESCRIPTION AND PARAMETRIC ANALYSIS

The analyzed reinforced system consists on a special hybrid cross-section, composed of intercalated layers of

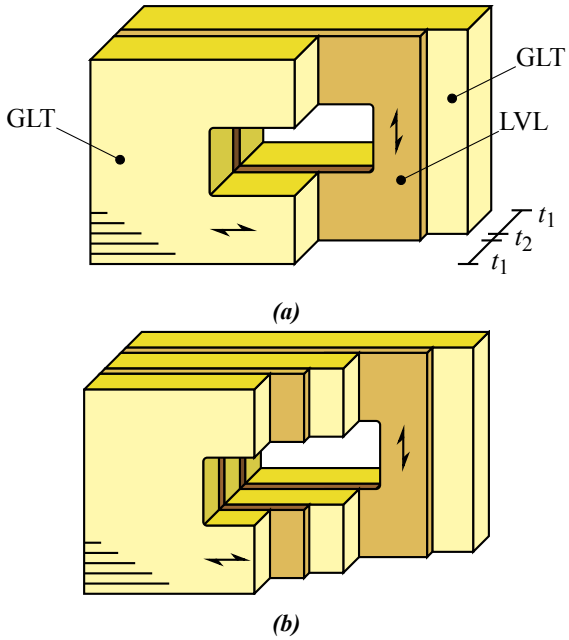

Figure 2: *General description of the analyzed internal reinforcement system in two different possible configurations: (a) a single LVL layer between two GLT elements and (b) two layers of LVL intercalated in-between three GLT elements.*

GLT and LVL, glued together along the width-direction of the beam (see Figure 2a). The cross-bonded layers with its fiber direction aligned perpendicular to main axis of the beam, are chosen in such quantity that they improve the mechanical properties of the structure in this direction significantly. On the other hand, the cross-bonded ratio is set as low as possible, in order not to reduce the lengthwise bending stiffness and strength too much, or even not at all The latter can obviously only be achieved by use of material/veneers of the LVL, which are significantly stronger than spruce GLT (such as beech). This arrangement confers a global strengthening character to the reinforcement, making it not only useful near the hole (locally), but throughout the whole length of the beam. This continuous, uninterrupted characteristic of the reinforcement makes it a good solution e.g. for beams with multiple (large) holes, since a single element serves simultaneously as reinforcement for all the holes.

Depending on the thickness of the needed cross-section, multiple layers of LVL and GLT can be used, helping to achieve a more efficient use of both materials (see Figure 2b). Nevertheless, the *optimal* configuration of thicknesses for a given number of layers and width of the beam is not a trivial task to solve—not always at least. For the case in which the system is mainly used as a reinforcement for holes, the percentage of the total tensile force $F_{t,90}$ that goes into each layer needs to be known, in order to perform the required design check at each layer. However, the composite build-up of the reinforced section, added to the complex stress redistribution in the hole-influenced region of the beam, complicates the determination of the load sharing between GLT and LVL. Different variables, like modulus of elasticity (MOE) perpendicular to the grain (E_{90}), layer thicknesses and section forces ra-

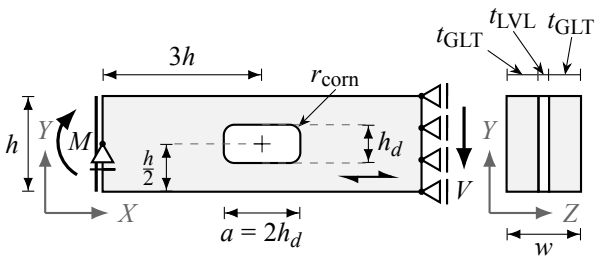

Figure 3: *Geometry and dimensions of the analyzed configurations; load application and boundary conditions used for the finite element model.*

tios, influence the redistribution of stresses in a complex manner. An analysis of the influence of these parameters is, hence, most desirable, since a practical use of the reinforcement requires an understanding of the effects of the different possible combinations. To this end, a parametric analysis was performed, which is described in the following section.

3.1 PARAMETRIC ANALYSIS

The analyzed configuration comprises the basic case, where only one LVL layer is inserted between two GLT beams, as shown in Figure 3. Three variables are investigated: (1) the elastic modulus perpendicular to the beam's axis of the reinforcement (LVL), (2) the thickness of the reinforcement, and (3) the ratio of moment-to-shear-force (M/V) in the region of the hole.

The beam has a depth of $h = 450$ mm and a total length of 2700 mm ($6h$), whereas the total width is set to be $w = 250$ mm. The thickness of the LVL layer (t_{LVL}) is varied between 15 mm and 50 mm in steps of 5 mm, while the thickness of the GLT elements (t_{GLT}) is accordingly adjusted to maintain the mentioned constant total width w. A rectangular hole with a fixed size $h_d \times a = 180 \times 360$ mm^2 is placed at mid-depth with its center at a distance of $3h = 1350$ mm from the next (here left) support. The used corner radius r_{corn} equals 20 mm.

The MOE perpendicular to the axis of the beam for the LVL, $E_{90,LVL}$, is studied for values between 300 N/mm^2 and 5000 N/mm^2 in steps of 600 N/mm^2, which, given $E_{90,GLT} = 300$ N/mm^2, gives MOE ratios $E_{90,LVL}/E_{90,GLT}$ from 1 to 15 in steps of 2. (Note: Physically, the different $E_{90,LVL}$ values stem from different cross-bonded ratios of the cross-bonded LVL) The shear-force V applied to the model remains constant for all the configurations, whilst the moment is varied by means of an externally introduced moment M at the position of the left support. Starting from zero, the external moment is increase in steps of 3×10^7 Nmm up to 9×10^7 Nmm, which translates into a total ratio M/V at the analyzed (right) edge of the hole of 1.53, 4.53, 7.53 and 10.53 [m].

4 DESCRIPTION OF THE FINITE ELEMENT MODEL

The finite element (FE) model was built using the software Abaqus v2017 [9] with its standard solver, using 3D continuum linear elements with reduced integration (element type: C3D8R). For the LVL, the size of the elements along the thickness (Z-direction) was chosen to be 5 mm, which ensures that for each consecutive thickness analyzed one extra layer of elements is created. Regarding the discretization of the GLT, an element thickness of 5 mm cannot be achieved for all configurations—due to some values not being multiples of 5—, but a close approximation was used, defined as $(t_{GLT}/\lceil t_{GLT}/5 \rceil)$ mm. This results in values of exactly 5 mm for LVL-thicknesses multiples of 10 and approximately 5 mm for the other cases. (Note: The objective to have the same discretization in both materials would require thicknesses of 2.5 mm, which would lead to a considerably increase in the computation time.) The side lengths of the elements contained in the XY-planes have a size of 4 mm directly on the periphery of the hole, increasing up to 10 mm on the region extending 180 mm to both sides of the hole's vertical edges (see Figure 4). After this, the size is progressively increased up to 30 mm.

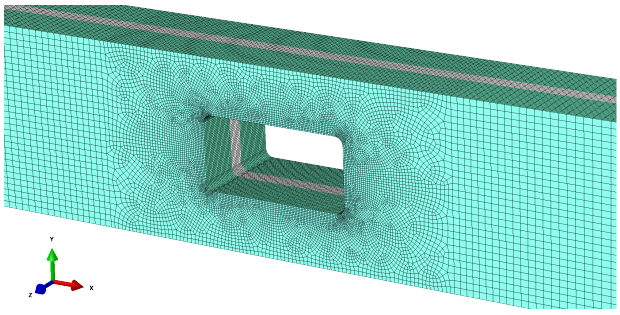

Figure 4: *Example of the meshing of the finite element model used for the parametric analysis. The different colors represent the regions with the two materials used; green: GLT material, gray: LVL material.*

Symmetry conditions are applied at one edge of the beam, according to Figure 3, where also a shear force $V = 50$ kN is applied. A rigid plane (element type: R3D4) is created on the side of the simple support, placed vertically in the YZ-plane, and is connected to the elements of the beam by means of *tie constraints*. The corresponding reference point is placed at the gravity center of the cross-section ($(y, z) = (h/2, w/2)$) and is used both to set the boundary conditions of the simple support and to apply the external moment M to the beam.

The material properties used for the LVL and GLT are presented in Table 1. For the LVL, the shear modulus (G_{xy}) was varied with a linear function, based on the value of E_{90}; it was set to have a value of 650 N/mm^2 at $E_{90,LVL} = 300$ N/mm^2 and 850 N/mm^2 for $E_{90,LVL} = 3900$ N/mm^2. For the solution of the model, no geometrical non-linearities were considered.

4.1 COMPUTATION OF THE TENSILE FORCE $F_{t,90}$

In order to numerically obtain the vertical tensile force $F_{t,90}$ from the results of the FE model, a horizontal path is defined at each Z-position where element nodes are

Table 1: *Material properties used for the finite element model*

Material	E_x	$E_{y/z}$	$G_{xy/xz}$	G_{yz}	$\nu_{xy/xz}$	ν_{yz}
	[N/mm^2]	[N/mm^2]	[N/mm^2]	[N/mm^2]	[–]	[–]
GLT	11500	300	650	65	0.02	0.2
LVL	11800	variable	$f(E_y)$	$G_{xy} \cdot 0.1$	0.02	0.2

present. The paths start at the corner 2 of the hole, subjected to tensile stresses perpendicular to the beam's axis, at an angle $\varphi = 45°$, as depicted in Figure 1, and extend for 400 mm. A numerical integration of the tensile stresses ($\sigma_{90} > 0$) is performed and the result is then multiplied by the thickness of the element (if it is between other elements) or by half of the thickness (if the path lays on one of the outer faces of each layer (GLT or LVL)). Finally, the values obtained in each layer are summed up and the total vertical tensile force for each layer is obtained.

5 RESULTS

The results from the FE-models were analyzed in order to gain some insight into the effect produced by the variation of each parameter on the structure. Following, the isolated influence of each one of the three analyzed parameters is presented. Firstly, the influence of the ratios of MOEs perpendicular to the beam's axis ($E_{90,\mathrm{LVL}}/E_{90,\mathrm{GLT}}$) is discussed. Secondly, the effect of the relative thickness of the LVL (t_{LVL}/w), and thirdly the impact produced by the different moment-to-shear-force ratios is revealed.

All the results were analyzed for corner 2 (see Figure 1), as in this region the tensile stresses, induced by the interaction of moment and shear-force, have their maximum effect. Note: on corner 1 the effect of the moment produces compressive stresses perpendicular to the grain and, thus, reduces the level of the vertical tensile force $F_{t,90}$ computed at this location.

5.1 EFFECT OF THE ELASTIC MODULUS PERPENDICULAR TO THE BEAM AXIS OF THE LVL

The effect of the MOE perpendicular to the main axis is presented in Figure 5 for $t_{\mathrm{LVL}} = 35\,\mathrm{mm}$ ($t_{\mathrm{LVL}}/w = 0.14$) and a moment-to-shear-force ratio $M/V = 1.53\,\mathrm{m}$. The horizontal x-axis shows the different MOE ratios investigated

$$\beta_E = \frac{E_{90,\mathrm{LVL}}}{E_{90,\mathrm{GLT}}}, \tag{2}$$

whilst the left vertical y-axis depicts the percentage of the force $F_{t,90}$ (bars) being taken up by the LVL element (η_{FE}). On the right vertical y-axis (orange dots) the values according to Eq. (3) are shown, which represent the LVL stiffness ratio vs. the total stiffness perpendicular to the grain:

$$\eta_{90,\mathrm{LVL}} = \frac{E_{90,\mathrm{LVL}} \cdot t_{\mathrm{LVL}}}{\sum_i E_{90,i} \cdot t_i} \tag{3}$$

Equation (3), representing a load sharing according to an ideal parallel spring/stiffness system, was chosen as a reference, since this is the direction in which the computed $F_{t,90}$ force is acting. In this sense, it should in theory reflect the behavior of the redistribution of stresses in the region of stress concentrations perpendicular to the beam's principal axis.

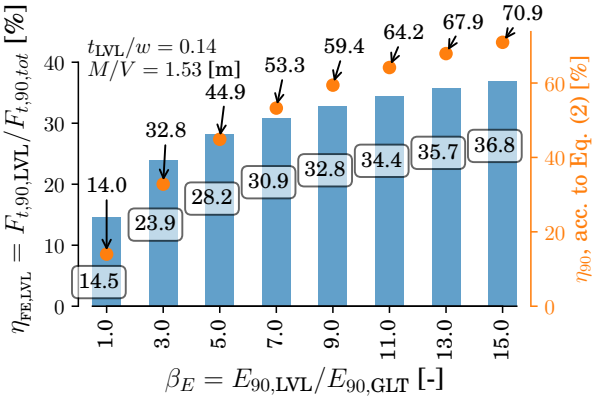

Figure 5: *Tensile force $F_{t,90}$ taken by the LVL as a function of the ratio of MOEs perpendicular to the beam's main axis $E_{90,LVL}/E_{90,GLT}$, for constant LVL/beam thickness ratio and moment-to-shear-force ratio. The bars (corresponding to the left y-axis) show the FE-results, while the orange dots (right y-axis) show the values according to Eq.* (3).

It can be observed from Figure 5, that the FE-results follow in principle a similar evolution as the one obtained with Eq. (3). However, only the scale differs, which indicates that the stresses do not have enough space to redistribute according to an ideal parallel system assumption. Coming from a rather bending-dominated cross-section, the internal forces are internally distributed based on the stiffnesses parallel to the axis of the beam, and only in a very close proximity of the corner they start to redistribute according to the stiffnesses perpendicular to the main axis. In this sense, the real load sharing is composed of a weighting of η_{90} on the one hand, and the theoretical load sharing parallel to the grain, η_0 on the other hand, (as proposed in [6])

$$\eta_{0,\mathrm{LVL}} = \frac{E_{0,\mathrm{LVL}} \cdot t_{\mathrm{LVL}}}{\sum_i E_{0,i} \cdot t_i}, \tag{4}$$

which means

$$\eta_{90,\mathrm{LVL}} = f\left(\eta_{90}, \eta_0\right). \tag{5}$$

The discussed behavior is observed in an exact manner for all the thicknesses and M/V ratios investigated. For this reason, the presentation of a single case is sufficient for the purpose of a general understanding. It is of importance to notice, that for the base case ($E_{90,\mathrm{LVL}}/E_{90,\mathrm{GLT}} = 1$), the FE-results conform very closely to the theoretical values, which should be equal to the thickness ratio. This

serves as a verification of the FE-model and the applied post-processing methodology.

5.2 EFFECT OF REINFORCEMENT THICKNESS

The influence produced by the variation of the thickness of the LVL layer is depicted in Figure 6 for a constant MOE ratio $E_{90,\mathrm{LVL}}/E_{90,\mathrm{GLT}} = 11$ and a constant M/V ratio of 1.53 m, i.e. equal to M/V in Figure 5. In the figure, the x-axis represents the different thickness ratios $\beta_t = t_{\mathrm{LVL}}/w$, whilst in the left and right y-axis the same variables as in Figure 5 are presented (percentage of $F_{t,90}$ in the LVL and η_{90} acc. to Eq. (3), respectively). The load sharing behavior obtained with the FE-model follows an almost perfectly linear relationship with increasing thickness ratios ($R^2 = 0.999$ for the observed case; compare also with Figure 7). This does not match with the predictions according to Eq. (3), which predicts a significantly higher nonlinear force relationship as for the previous case.

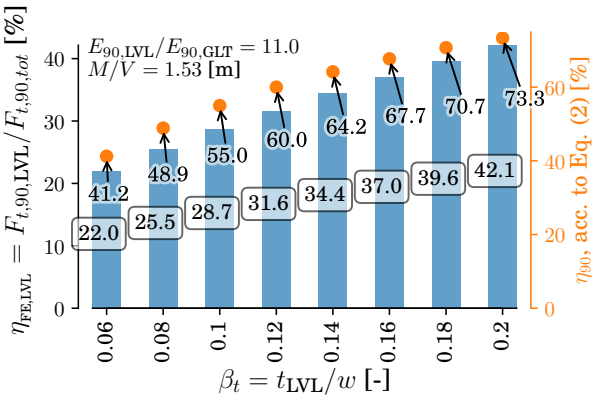

Figure 6: *Tensile force $F_{t,90}$ taken by the LVL as a function of the relative thickness of the LVL plate. The bars (corresponding to the left y-axis) show the FE-results, while the orange dots (right y-axis) show the theoretical values according to Eq.* (3).

An analysis of the configurations with different MOE ratios shows that this linear relationship is present in all the studied cases. Figure 7 shows the different percentages of total $F_{t,90}$ in the LVL for the stiffness ratios (η_{FE}) used in the parametric study, and makes the mentioned linearity evident by showing the R^2 values. This effect is expressed for all the ratios M/V as well, reason for which the presentation of a single case is deemed sufficient.

The phenomenon observed here can be explained by the fact that, added to the previous mentioned effects, the LVL layer has a limited area of influence to its sides regarding the redirection of load/stresses on the width direction (z-direction), which does not evolve at the same rate as its thickness. This can be observed in Figure 8, where the stresses perpendicular to the beam's axis, σ_{90}, are plotted vs. the width, i.e. z-direction, at an angle of 45°. The distance of influence of the LVL layer is a nonlinear function, and adds up to the deviation from the analytical Eq. (4). Additionally, it can be seen in Figure 8 that the stresses σ_{90} exhibit a large variation within the thickness of the LVL, having a peak at the surface in contact with the GLT, then decreasing parabolically to the mid-thick of the plate. A

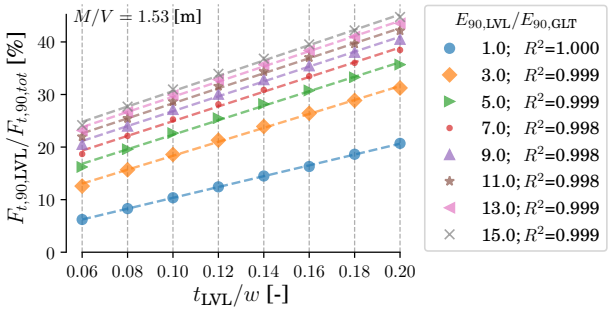

Figure 7: *Tensile force $F_{t,90}$ taken by the LVL as a function of the thickness ratio of the LVL, for different MOE ratios. The linear regression for the MOE ratios are represented by the dashed lines and their R^2 values are displayed on the right legend.*

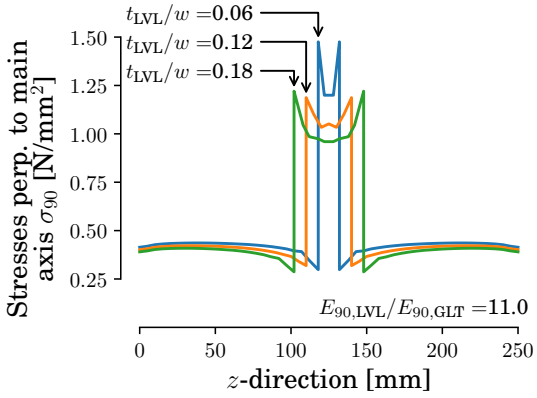

Figure 8: *Stresses perpendicular to the main axis of the beam, obtained under 45° at corner 2 for three different ratios LVL to beam widths. The presented path crosses the three different layers (GLT-LVL-GLT). The effect of the thickness of the LVL on the GLT stresses is depicted.*

detailed investigation of these two effects are outside of the scope of this paper, but the respective influences will be taken into account by means of a coefficient, when trying to obtain an analytical equation for the load sharing of the system.

5.3 EFFECT OF THE MOMENT-TO-SHEAR-FORCE RATIO M/V

A study of the parameters "moment-to-shear-force ratio" (M/V) is relevant, since the internal forces in the region containing the hole are expected to have an effect in the mentioned weighting of the load shares η_{90} and η_0. Figure 9 presents the FE-results for a constant thickness ratio $t_{\mathrm{LVL}}/w = 0.14$. The x-axis shows the different MOE ratios, whilst the y-axis presents the percentage of the force $F_{t,90}$ in the LVL. An interesting behavior is observed when comparing the effect of the ratio M/V for different MOE ratios: while for $\beta_E < 5$ a higher M/V ratio produces a decrease of the tensile force taken by the LVL (η_{FE}), the opposite happens for $\beta_E > 5$, i.e. η_{FE} grows with higher moment-to-shear-force ratios.

This phenomenon can be further analyzed by performing a linear regression on each set of results with different MOE ratios. This is, for every group of ratios M/V corre-

sponding to the same thickness and MOE ratio (e.g. first four columns of the Figure 9) the slope is computed. Since the percentage of the tensile force $F_{t,90}$ that is taken by the LVL was defined as

$$\eta_{\text{FE,LVL}} = \frac{F_{t,90,\text{LVL}}}{F_{t,90,tot}}, \tag{6}$$

the slope needed is the partial derivative of $\eta_{\text{FE,LVL}}$ with respect to (M/V), i.e.

$$\theta = \frac{\partial \eta_{\text{FE,LVL}}}{\partial (M/V)}. \tag{7}$$

Figure 10 presents the values of the slope θ, normalized by the MOE ratio β_E, for different thickness ratios β_t, as a function of the MOE ratio. This figure confirms the initial observation regarding the effect of the moment-to-shear-force ratio, since a negative slope is observed for all the thickness ratios when $\beta_E < 5$ (shaded area). The second, and more relevant information, consists in the fact that, the curve, i.e. the section force ratio effect on $\eta_{\text{FE,LVL}}$, obtained for all the configurations with $\beta_E > 5$ behave in a similar manner.

5.4 ANALYTICAL ASSESSMENT OF THE LOAD SHARING RATIO

With the gathered information from the previous sections, an analytical model for the computation of the load share between LVL and GLT of the tensile force $F_{t,90}$ will be presented. In essence, the proposed model considers the determination of an effective thickness, t_{eff} (Eq. (8)), and an effective MOE perpendicular to the grain for the LVL, $E_{90,\text{eff}}$ (Eq. (9)), which are then used to compute the values η_{90} and η_0 according to Eqs. (3) and (4), respectively. (Then: $E_{90,\text{LVL}} = E_{90,\text{eff,LVL}}$ and $t_{\text{LVL}} = t_{\text{eff,LVL}}$.) These two values are weighted (parameter p_3 (see Eq. 10)) and then multiplied by a factor dependent on the M/V ratio (Eq. (10)). The model contains four parameters p_1 to p_4 to be derived from an optimization procedure (see below), and takes the following form:

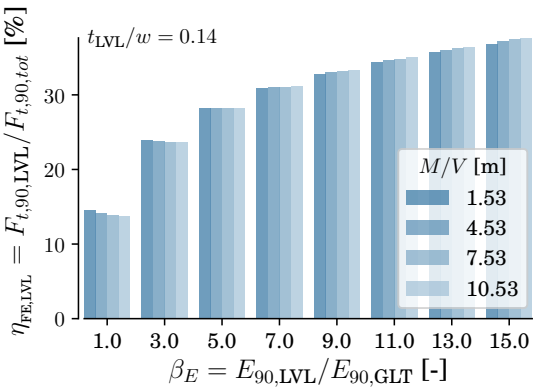

Figure 9: *Tensile force $F_{t,90}$ taken by the LVL as function of the ratio of MOEs perpendicular to the axis of the beam $E_{90,LVL}/E_{90,GLT}$. The force ratios are specified for different moment-to-shear-force ratios M/V.*

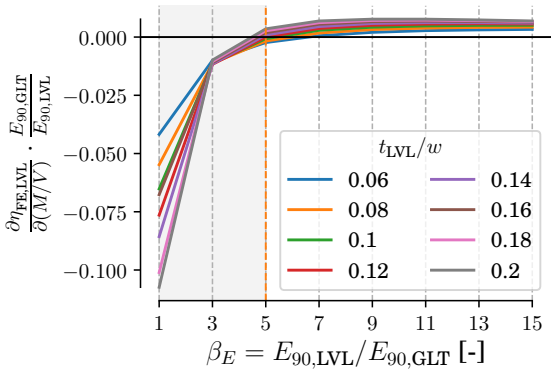

Figure 10: *Dependency of $F_{t,90}$ share on different ratios M/V (θ), normalized by the MOE ratio $E_{90,LVL}/E_{90,GLT}$, plotted against the stiffness ratio. All the studied thickness ratios are presented as well.*

$$t_{\text{eff}} = (t_{\text{LVL}})^{p_1} \tag{8}$$

$$E_{90,\text{eff}} = E_{90,\text{LVL}} \cdot (\beta_E)^{p_2} \tag{9}$$

$$\eta_{\text{analyt}} = [\eta_{90} \cdot p_3 + \eta_0 \cdot (1 - p_3)] \cdot \gamma_M \tag{10}$$

$$\gamma_M = \left(\frac{M}{V}\frac{1}{\beta_E}\right)^{p_4}. \tag{11}$$

It is important to notice that in the computation of η_{90} and η_0 only the variables corresponding to the LVL have to be changed, i.e. thickness and $E_{90,\text{GLT}}$ remain the same. In addition, it has to be noticed that the unit of the moment-to-shear-force is in [m].

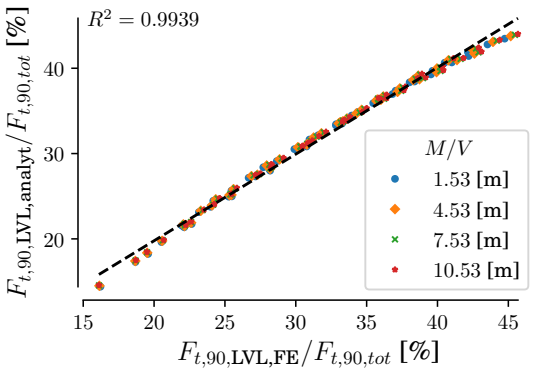

Figure 11: *Linear regression (dashed line) of all the analyzed data used for the calibration of the model. The individual data for the FE-results and analytical model are shown as scattered dots, differenced by color for their moment-to-shear-force ratio.*

The model (η_{analyt}) was calibrated with the data obtained from the parametric analysis ($\eta_{\text{FE,LVL}}$), by means of an optimization process based on the least-square-roots method. To this end, a function was written using Python and its scientific library SciPy [10], which contains the needed optimization algorithms. For the calibration process, only the results for MOE ratios $\beta_E \geq 5$ were considered, as it was shown that for the lower ratios the effect of the moment-to-shear-force ratio has the contrary effect on

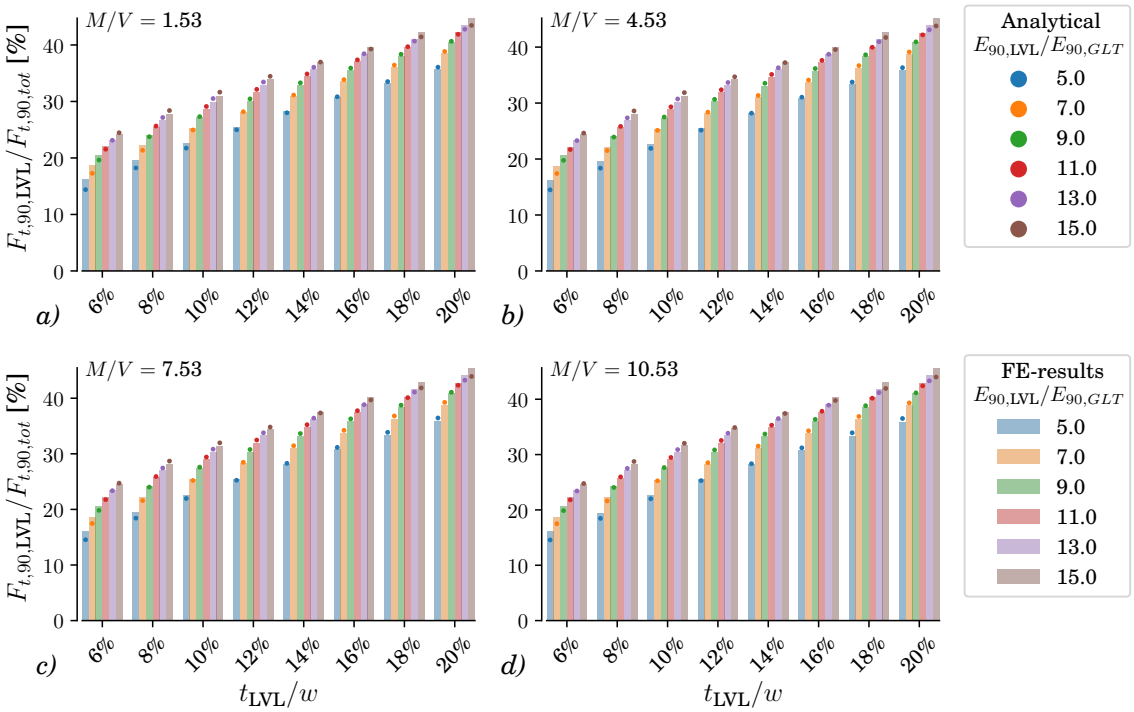

Figure 12: *Comparison of the FE-results ($\eta_{FE,LVL}$) and values obtained with the calibrated analytical model (η_{analyt}) regarding the $F_{t,90,LVL}$ load ratio. The subplots (a)-(d) relate to different moment-to-shear-force ratio.*

the load sharing, and is therefore not trivial to model with an analytical equation. Nevertheless, the authors are of the opinion that for the investigated use case, lower ratios of MOEs perpendicular to the beam axis are of little relevance, since a reinforcement of the cross-section in this direction requires a relatively high MOE value.

Table 2: *Parameters obtained through the optimization process for the analytical model*

p_1	p_2	p_3	p_4
1.021	0.135	0.346	0.00647

The results from this process are presented in Figure. 11 and 12, and the obtained parameters p_1, p_2, p_3 and p_4 are given in Table 2. Figure 12 shows the percentage of the force $F_{t,90}$ taken by the LVL, computed both by means of the FE-results (bars) and by the calibrated analytical model (dots). It can be observed that for all the studied cases a satisfactory agreement between the FE-results and analytical model is achieved. In other words, the proposed model is adequate to represent the load sharing of the tensile force $F_{t,90}$ between LVL and GLT.

Figure 11 depicts the results of a linear regression between all the FE-obtained results for the load sharing and the corresponding analytical ones. From the figure, it can be seen that a good correlation between both values is observed, which is represented by an R^2 value of 0.994. Nevertheless, the fit is not perfect, and some values (mostly for the extremes of the thickness ratios analyzed) express some differences with the FE-results (up to 11 %, but normally moving around 1 %).

6 CONCLUSIONS

The parametric study of the GLT-LVL composite shows that the load share for the vertical tensile force $F_{t,90}$ is a non-trivial value to obtain. The analyzed parameters showed that

- a load sharing purely based in the stiffness ratios perpendicular to the grain, η_{90}, does not fully explain the numerical results. Due to the relatively short distance ahead of the hole, in which the stresses are redistributed to produce the tensile stress concentrations at the corners, the redistribution according to the theory is only partially fulfilled. Moreover, the *real* load share is bound to a weighted combination of η_{90} and η_0.
- A change in the ratios of elastic modulus perpendicular to the main axis of the beam produces a similar-shaped curve as the theoretical η_{90} does, however, a difference in scale is observed. However, a change in the thickness ratio is characterized by a rather linear behavior, which is not explained by the theoretical η_{90}. The most relevant reason is the decaying influence of the LVL on the GLT with increasing distance in the width direction; also, there is a large variation of the stresses within the LVL, which seems to get stronger with thicker cross-sections.
- The moment-to-shear-force ratio has a very complex influence in the load sharing of the tensile force $F_{t,90}$, producing a decrease in the load sharing for MOE ratios smaller than 5, and increasing the same value for MOE ratios larger than 5. Nevertheless, since

the expected use as a reinforcement requires relative high MOE ratios, this effect can be ignored and assume that a higher M/V ratio will produce higher load shares.

- Based on the observations made during the analysis of the results, an analytical model for the computation of the loading share was developed. The model considers modifications for the thickness and MOE values of the LVL, which are used to compute the theoretical load shares η_{90} and η_0; after this, both values are weighted and multiplied by a factor dependent on the moment-to-shear-force.

- The calibrated model is able to reproduce the finite element results in a good manner, exhibiting relative small errors of about 1%.

- The model parameters p_1–p_4 were calibrated to FE results for a specific rectangular hole configuration, with a hole-to-depth ratio of 0.4 and a hole aspect ratio (length/depth) of 2. Further hole configurations shall be studied to assure the generality of the chosen approach.

REFERENCES

[1] DIN EN 1995-1-1/NA, *National Annex – Nationally determined parameters – Eurocode 5: Design of timber structures – Part 1-1: General – Common rules and rules for buildings*, German Institute for Standardization, Berlin, Germany, 2013.

[2] S. Aicher and C. Tapia, "Glulam with laterally reinforced rectangular holes," in *World Conference on Timber Engineering*, Auckland, New Zealand, 2012.

[3] M. Danzer, P. Dietsch, and S. Winter, "Reinforcement of round holes in glulam beams arranged eccentrically or in groups," in *CD-ROM Proceedings of the World Conference on Timber Engineering (WCTE 2016)*, J. Eberhardsteiner, W. Winter, A. Fadai, and M. Pöll, Eds., Vienna, Austria: Vienna University of Technology, Austria, 2016, ISBN: 978-3-903039-00-1.

[4] C. Tapia and S. Aicher, "Holes in glulam – Orientation and design of internal reinforcements," in *CD-ROM Proceedings of the World Conference on Timber Engineering (WCTE 2016)*, J. Eberhardsteiner, W. Winter, A. Fadai, and M. Pöll, Eds., Vienna, Austria: Vienna University of Technology, Austria, 2016, ISBN: 978-3-903039-00-1.

[5] T. Butler, "International house sydney," in *Proceedings (Part II) 22nd. Wood Construction Forum (IHF 2016)*, Garmisch, Germany, 2016, pp. 35–45.

[6] S. Aicher and C. Tapia, "Novel internally LVL-reinforced glued laminated timber beams with large holes," *Construction and Building Materials*, vol. 169, pp. 662–677, 2018, ISSN: 0950-0618. DOI: 10.1016/j.conbuildmat.2018.02.178.

[7] S. Aicher and L. Höfflin, "Runde Durchbrüche in Biegeträgern aus Brettschichtholz. Teil 1: Berechnung," *Bautechnik*, vol. 78, no. 10, pp. 706–715, 2001.

[8] C. Tapia and S. Aicher, "Improved design equations for the resultant tensile forces in glulam beams with holes," in *International Network on Timber Engineering Research — Meeting 50*, Kyoto, Japan, 2017.

[9] Abaqus v2017, Dassault Systèmes Simulia Corp, Johnston, RI, USA, 2017.

[10] E. Jones, T. Oliphant, P. Peterson, *et al.*, *SciPy: Open source scientific tools for Python*, [Online; accessed 2018-04-25], 2001–. [Online]. Available: http://www.scipy.org/.